

Research Article

A perfusion bioreactor system efficiently generates cell-loaded bone substitute materials for addressing critical size bone defects

Claudia Kleinhans^{1,2,*}, Ramkumar Ramani Mohan^{3,4,*}, Gabriele Vacun⁴, Thomas Schwarz⁴, Barbara Haller⁵, Yang Sun⁶, Alexander Kahlig¹, Petra Kluger^{4,7}, Anna Finne-Wistrand⁶, Heike Walles^{3,4} and Jan Hansmann^{3,4}

¹ Institute for Interfacial Process Engineering and Plasma Technology IGVP, University of Stuttgart, Stuttgart, Germany

² Department of Orthopedics, Medical University Graz, Graz, Austria

³ Chair Tissue Engineering and Regenerative Medicine, University Hospital Wuerzburg, Wuerzburg, Germany

⁴ Fraunhofer Institute for Interfacial Engineering and Biotechnology, Stuttgart, Germany Department

⁵ FH Esslingen, Esslingen am Neckar, Germany

⁶ Department of Fibre and Polymer Technology, KTH Royal Institute of Technology, Stockholm, Sweden

⁷ University Reutlingen, Process Analysis & Technology (PA&T), Reutlingen, Germany

Critical size bone defects and non-union fractions are still challenging to treat. Cell-loaded bone substitutes have shown improved bone ingrowth and bone formation. However, a lack of methods for homogeneously colonizing scaffolds limits the maximum volume of bone grafts. Additionally, therapy robustness is impaired by heterogeneous cell populations after graft generation. Our aim was to establish a technology for generating grafts with a size of 10.5 mm in diameter and 25 mm of height, and thus for grafts suited for treatment of critical size bone defects. Therefore, a novel tailor-made bioreactor system was developed, allowing standardized flow conditions in a porous poly(L-lactide-co-caprolactone) material. Scaffolds were seeded with primary human mesenchymal stem cells derived from four different donors. In contrast to static experimental conditions, homogenous cell distributions were accomplished under dynamic culture. Additionally, culture in the bioreactor system allowed the induction of osteogenic lineage commitment after one week of culture without addition of soluble factors. This was demonstrated by quantitative analysis of calcification and gene expression markers related to osteogenic lineage. In conclusion, the novel bioreactor technology allows efficient and standardized conditions for generating bone substitutes that are suitable for the treatment of critical size defects in humans.

| | |
|-------------------------|-------------|
| Received | 03 DEC 2014 |
| Revised | 20 MAR 2015 |
| Accepted | 19 MAY 2015 |
| Accepted article online | 26 MAY 2015 |

Keywords: Bone substitute · Critical size defect · Perfusion bioreactor system · Poly(LLA-co-CL) scaffold · Tissue engineering

Correspondence: Dr. Jan Hansmann, Chair Tissue Engineering and Regenerative Medicine, University Hospital Wuerzburg, Roentgenring 11, 97070 Wuerzburg, Germany

E-mail: Jan.Hansmann@uni-wuerzburg.de

Abbreviations: CAD, computer-aided design; DMEM, Dulbecco's Modified Eagle's Medium; FACS, fluorescence activated cell sorting; FCS, fetal calf serum; g_0 , standard acceleration due to gravity; hMSCs, human mesenchymal stem cells; MTT, 3-(4,5-dimethylthiazol-2-yl)-2,5-Diphenyltetrazolium bromide; P(LLA-co-CL), poly(L-lactide-co-caprolactone); PBS, phosphate buffered saline; qRT-PCR, quantitative real time polymerase chain reaction; SEM, scanning electron microscopy; TGF β 3, transforming growth factor β 3

1 Introduction

Critical bone defects, caused by i.e. resection of tumor tissue or infectious tissue as well as trauma surgeries, are still challenging to treat. Currently, a few million patients per year require a bone graft or bone graft substitute to cure bone defects and diseases [1]. Mostly, autografts, allografts, or synthetic materials are used to bridge a critical defect that is exceeding the natural healing capacity

* These authors contributed equally to this work.

of native bone tissue. Due to a lack of autologous material, the risk of donor site morbidity, or transmission of diseases by using allogenic and xenogenic grafts, the development of substitute materials for treatment of critical size bone defects is essential [2]. It has been shown that implantation of cell-loaded materials or in vitro pre-seeded scaffolds resulted in enhanced bone formation and bone bonding in vivo [3, 4]. Thus, combining synthetic materials and autologous cells – ideally obtained by the patient himself – in a tissue engineering process provides a possibility to generate an implant that exhibits physiological characteristics of human bone and enhances bone formation and graft ingrowth [5]. The requirements of generating artificial bone tissue are suitable scaffolds, multipotent stem cells, i.e. human mesenchymal stem cells (hMSCs), and culture conditions that facilitate the nourishment of cells in a three-dimensional (3D) construct. A scaffold material for bone regeneration should feature a high porosity – to allow cell migration –, biodegradability and osteoconductivity [6]. Currently, a broad range of synthetic materials are used for bone grafting; mostly manufactured of ceramics like beta-tricalcium-phosphates (β -TCP) and hydroxyapatite [7], polymers such as polylactide or polyethylene [8], or composite materials [9]. The poly(L-lactide-co-caprolactone) (P[LLA-co-CL]) used in this study has already been reported to fulfill requirements for improved bone formation [10, 11]. However, an efficient and standardized process that is applicable in a GMP-conform environment for generating a cell-loaded bone substitute still needs to be developed.

A tissue culture process is usually composed of scaffold seeding – when cells are distributed throughout the material – and the culture/maturation of the construct. In standard static culture conditions, mass transport is driven by diffusion. It has been shown that diffusion processes in tissues are limited to a distance of approximately 200 μm , and are therefore insufficient to appropriately supply cells within the core of a large 3D tissue constructs [12]. In addition to limited nutrients supply during tissue culture, it has been demonstrated that hMSCs respond to the culture conditions, such as fluid shear stress, which stimulates the production of specific markers, e.g. extracellular matrix proteins [13, 14]. Thus, a process for generating bone grafts should ensure sufficient nutrients supply and support specific lineage differentiation. For maintaining controlled culture conditions, bioreactors are employed. Several bioreactor systems such as spinner flask-, rotating wall vessel- or perfusion bioreactors were developed to overcome nutrient limitations, and in addition, to provide mechanical stimuli of the cells [15–19]. Nevertheless, most of these systems exhibit heterogeneous mechanical stimulation, require extensive culture duration, or need complex technical setup.

The novel perfusion bioreactor presented here ensured robust process conditions based on a simple sealing concept, which was derived employing computation-

al modeling. The perfusion system allowed homogeneous cell distribution and significant osteogenic lineage commitment of hMSCs after one week of culture without addition of soluble factors for inducing osteogenic differentiation. Furthermore, the bioreactor met the requirements for the culture of bone substitutes, which can be applied in the treatment of critical size bone defects in humans.

2 Materials and methods

2.1 Polymer scaffold fabrication

According to a previously published protocol, P(LLA-co-CL) was synthesized by random ring-opening-polymerization catalyzed by stannous 2-ethylhexanoate ($\text{Sn}[\text{Oct}]_2$) with a monomer/catalyst mole ratio of 10 000:1 [10]. The resulting co-polymers consisted of 75 mol% L-lactide and 25 mol% of ϵ -caprolactone, verified by proton nuclear magnetic resonance (^1H NMR). Porous 3D scaffolds were prepared by solvent casting and salt leaching method. Sodium chloride particles with a range of particle size of 90–500 μm were used as the porogen. The salt-polymer blend was loaded into 15 \times 45 mm glass vials (VWR, Stockholm, Sweden) for moulding. Scaffolds were salt-leached after solvent evaporation, polished and sized to about 10.5 mm diameter and approximately 25 mm in length.

2.2 Computational fluid dynamic

To predict the shear stress distribution in the porous scaffold, computational modeling was performed. Therefore, three domains – an inlet, an outlet, and the porous scaffold – were generated according to the bioreactor cartridge geometry employing computer-aided design (CAD). To simulate the flow regimes, COMSOL Multiphysics™ was used. The in- and outlet were defined as laminar flow domains, whereas, Darcy's law derived for creeping flows, i.e. for Reynolds numbers $Re \ll 1$, was applied for the porous scaffold. At a flow rate of 0.8 mL/min, Re was approximately 214 $[1/\text{m}] \times$ pore diameter [m], in our system. Thus, with pore diameters in the range of micrometers, Re was $\ll 1$ and Darcy's law held. The porosity of the scaffold was set as 90%, according to the μCT data. By measuring the pressure difference at different flow rates, the permeability of the scaffold was determined as $1.72 \pm 0.2 \times 10^{-1} \text{ m}^2$. At the inlet, a total flow of 0.8 mL/min was defined as boundary condition. The outlet was set to ambient pressure.

2.3 Isolation and culture of primary human mesenchymal stem cells (hMSCs) from bone marrow aspirate and femur head biopsies

hMSCs were isolated with approval of the local ethics committee (vote IGBZSF-2012-078, vote 182/10) from

bone marrow aspirate (Lonza, Walkersville, USA) of two male 24 and 25 years old, and one female 45 years old healthy donors, or from femur head biopsies (male, 76). Briefly, bone marrow aspirate was diluted 1:1 with phosphate buffered saline containing calcium and magnesium (PBS⁺), and 20 mL of the suspension were gently layered over 15 mL Biocoll (Biochrom AG, Berlin, Germany). Centrifugation was performed at $400 \times g_0$ (Heraeus Multifuge 3 R-S, Thermo Fisher Scientific, Schwerte, Germany) for 20 min at room temperature. The mononuclear cell layer was removed, and PBS⁺ containing 0.5% v/v fetal calf serum (FCS) from Lonza (Verviers, Belgium) was added. Following a further centrifugation step ($400 \times g_0$ for 7 min), supernatant was removed and growth medium composed of MSCGM™ Bullet Kit™ (Lonza, Verviers, Belgium) supplemented with 2% v/v FCS, 50 units/mL penicillin, and 50 µg/mL streptomycin from Life Technologies (Darmstadt, Germany) was added. For cell isolation from femur head biopsies, cells were washed in Dulbecco's Modified Eagle's Medium (DMEM, Biochrom AG, Berlin, Germany), gently agitated, and centrifuged at $300 \times g_0$ following the removal of spongiosa. Then, fat tissue was discarded from the supernatant and the suspension was transferred to a new centrifugation tube that was occupied with 15 mL DMEM (Biochrom AG). Cells of both biopsies were seeded into culture flasks after a further centrifugation step at $400 \times g_0$ (bone marrow aspirate) or $300 \times g_0$ (femur head biopsies) for 5 min. After 72 h incubation at 37°C in a 5% CO₂ humidified atmosphere, non-adherent cells were removed. For harvesting, cells were washed with phosphate buffered saline without calcium and magnesium (PBS⁻), and 0.05 mL/cm² 0.05% v/v trypsin/EDTA in Versene (Life Technologies) was added. Following incubation for 2 min at 37°C, the enzymatic reaction was halted by addition of FCS and cells were recovered after a centrifugation step (5 min at $200 \times g_0$; at room temperature).

2.4 Cell differentiation

To show multipotency of isolated hMSCs, adipogenic, osteogenic, and chondrogenic differentiation was induced by medium supplementation. As negative control, cells were cultured in proliferation medium composed of DMEM, 10% v/v FCS, 50 units/mL penicillin, and 50 µg/mL streptomycin (Life Technologies). Analysis was performed with a light microscope Eclipse TS100 (Nikon, Duesseldorf, Germany).

2.4.1 Adipogenic differentiation

hMSCs were plated in four-well Permanox® chamber slides (Nunc, VWR, Darmstadt, Germany) at a density of 30 000 cells/cm². After 3 days of culture, adipogenic differentiation was induced by using proliferation medium supplemented with 1 µM dexamethasone, 500 µM 3-Isobutyl-1-methylxanthine, 1 µg/mL insulin, 100 µM

indomethacin (all chemicals from Sigma-Aldrich, Munich, Germany) for 14 days. Medium was changed twice a week.

2.4.2 Chondrogenic differentiation

A pellet of 250 000 cells was generated by centrifugation for 5 min at $200 \times g_0$ (Multifuge 3 R-S, Heraeus). Cell pellets were cultured in 1 mL proliferation medium supplemented with 50 µg/mL ascorbate-2-phosphate, 100 nM dexamethasone, 100 µg/mL pyruvate, 40 µg/mL L-proline, 1% v/v insulin-transferrine-selenite (all chemicals from Sigma-Aldrich) and 10 ng/mL TGFβ₃ (R&D Systems, Wiesbaden, Germany) for four weeks. Medium was changed twice a week.

2.4.3 Osteogenic differentiation

Cells were seeded in a density of 3×10^4 cells/cm². Osteogenic differentiation was induced by switching to proliferation medium supplemented with 50 µg/mL L-ascorbic acid 2-phosphate, 10 mM β-glycerophosphate, 100 mM dexamethasone (all chemicals from Sigma-Aldrich). Medium was changed three times a week for 28 days.

2.5 Oil red O staining

Evaluation of adipogenic differentiation was performed by staining of accumulated intracellular lipid droplets. Therefore, cells were washed with PBS⁺ and fixed with Histofix® (Roth, Karlsruhe, Germany) for 10 min. Following two washing steps (PBS⁺ and aqua dest.), and permeabilization with 60% v/v isopropanol for 5 min, staining was conducted with oil red O solution (0.3% w/v oil red O from Sigma-Aldrich in 60% v/v isopropanol). For counter staining, Mayer's Haemalum solution (Fluka via Sigma-Aldrich) was applied. Subsequently, samples were rinsed with water and covered with Aquatex® (Merck Millipore, Darmstadt, Germany).

2.6 Analysis of chondrogenic differentiated cell pellets

Cell pellets were washed with PBS⁺ and fixed with Histofix® for 1 h. After paraffin embedding, 3 µm histological sections of the samples were generated, employing a microtome (Leica RM 2145, Wetzlar, Germany).

2.6.1 Alcian blue staining at pH 1.0

For visualization of proteoglycans, which are abundant in cartilage, Alcian blue staining was performed. Sections were heated for 30 min at 60°C, and subsequently, deparaffinized using Roticlear® (Roth) and decreasing ethanol concentrations. Washing in 0.1 M HCl was performed for equilibration. Alcian blue solution containing 1% w/v alcian blue 8GX (Sigma-Aldrich) in 0.1 M HCl was applied. For counter staining, nuclear fast red solution (5%

w/v aluminiumsulfate, 0.1% w/v nuclear fast red, in aqua dest.) was used to visualize cell nuclei (all chemicals from Sigma-Aldrich). After dehydrating, sections were covered with isomount® (VWR).

2.6.2 Antibody staining (collagen II)

Histological sections were heated for 15 min at 60°C after deparaffinizing the samples using Roticlear® and decreasing concentrations of ethanol. This was followed by digestion with pronase (Roche Diagnostics, Mannheim, Germany), and incubation with 3% v/v H₂O₂ to inactivate the cellular peroxidase. Samples were incubated with blocking buffer for the reduction of unspecific binding. Incubation with primary antibody (mouse monoclonal, clone II-4C11, Acris Antibodies GmbH, Herford, Germany) was done in a dilution of 1:600 at 4°C overnight. As secondary antibody, a multilink antibody (DCS Innovative Diagnostik Systeme, Hamburg, Germany) was applied in a dilution of 1:300. As substrate, AEC-Chromogen (DCS Innovative Diagnostik Systeme) was used. Nuclei were stained with Mayer's Haemalaun. Finally, sections were covered with Aquatex® (Merck Millipore).

2.7 Alizarin red staining

Calcification was detected by staining of calcium depositions with alizarin red. Therefore, samples were washed with PBS⁻ and fixed with Histofix® for 10 min. Cells were stained with alizarin red solution containing 1% w/v alizarin red S and 0.25% v/v ammonia, pH 6.3–6.4 (both chemicals from Sigma-Aldrich) for 30 min, and subsequently, rinsed with water.

2.8 Calcification assay

The protocol for the calcification assay was adopted from Raeth et al. [20]. For staining of 3D scaffolds, cells were fixed with 50% EtOH for 20 min and stained in 1% w/v alizarin red (Sigma-Aldrich) at pH 6.3–6.4 for 30 min under continuous shaking. Subsequently, cells were rinsed three times with aqua bidest. For quantification of the calcium content, the dye was solved with a solution containing 0.5 M HCl (Sigma-Aldrich) and 5% w/v sodium dodecyl sulfate (Sigma-Aldrich) for 30 min at room temperature. Absorbance of the solvent was measured in a plate reader at 415 nm (Infinite M200, Tecan).

2.9 Fluorescence-activated cell sorting analysis

Fluorescence-activated cell sorting (FACS) was applied to profile the expression pattern, using antibodies against CD73 (BD, Heidelberg, Germany), CD90, CD105, CD14, CD19, CD34 and CD45 (all from Beckman Coulter, Krefeld, Germany). Cells were diluted in stain buffer (FBS, BD Pharmingen, Heidelberg, Germany), and 2×10^5 cells were stained with 1 µg of antibody by incubation for

20 min at room temperature. Cells without antibody and an isotype control against IgG1 were used as negative control.

2.10 Immunofluorescence staining of actin and vinculin

Samples were fixed in Histofix® for 10 min and permeabilized with 0.1% w/v Triton X 100 (Sigma-Aldrich) in PBS⁺ for 10 min. Following, samples were rinsed three times in PBS⁺ for 2 min and incubated with primary antibody solution containing vinculin-FITC-conjugated 1:50 (Sigma-Aldrich) and phalloidin Alexa Fluor® 546 (Life Technologies) in a dilution of 1:50 for 60 min. Subsequently, cells were washed in PBS⁺ and mounted with ProLong Gold® with DAPI (Life Technologies).

2.11 Bioreactor system

The bioreactor system was composed of a medium reservoir, filled with 30 mL of growth medium (MSCGM™ Bullet Kit™ supplemented with 2% v/v FCS, 50 units/mL penicillin, and 50 µg/mL streptomycin), and the bioreactor cartridge, which was harboring the scaffold inside a silicone housing. A sampling port (Fenwal, Munich, Germany) was incorporated for cell seeding and medium change. To provide standardized pressure conditions, a pressure sensor was installed at the inlet of the bioreactor cartridge. Inside the cartridge, the silicone tube with an inner diameter of 11 mm sealed the scaffold during the experiments. Therefore, the construct inside the tubing was mounted on a clamp that pressed the silicone tube onto the cylinder jacket surface of the scaffold. Lids on both ends were prepared with tube connectors for fluidic bearing. Fluid flow was maintained by a peristaltic pump (ISMATEC, Wertheim, Germany).

2.12 Seeding of the scaffold material

Biodegradable porous Poly(LLA-co-CL) cylinders were seeded under dynamic condition in the perfusion bioreactor. Scaffolds were placed in the custom-fit notch of the bioreactor cartridge and perfused by a peristaltic pump for 1 h with cell culture medium. hMSCs were harvested and suspended in growth medium to a concentration of 5×10^5 hMSCs/mL. 10 mL of cell suspension was transferred to a 10 mL syringe and was injected air-bubble-free through the sterile sampling port with a syringe pump (Landgraf Laborsysteme, Langenhagen, Germany) with a flow rate of 0.5 mL/min. Applied pressure was monitored by the pressure sensor and controlled to 10–20 mmHg. Then, cell suspension was pumped through the bioreactor chamber in alternating cycles for 10 s forward and 3 s backward at total of 1 h at 1.6 mL/min. Following, the pump was stopped for 30 min to allow cell adhesion.

2.12.1 Dynamic culture

For culture, seeded scaffolds were perfused in the bioreactor four times per hour for 5 min at 0.8 mL/min. The total culture duration was either one day or seven days at 37°C and 5% CO₂. On day one and day four, 25 mL cell culture medium was exchanged. During culture, no further hMSCs were introduced into the system.

2.12.2 Static culture

As a control, seeded scaffolds were cultured in static culture conditions. Therefore, dynamically seeded constructs were transferred from the bioreactor into a 50 mL sterile glass bottle equipped with a 0.22 µm filter (Sartorius, Goettingen, Germany) for gas exchange, and cultured in growth medium at 37°C and 5% CO₂. 25 mL medium was exchanged on day one and four, analogously to the dynamic culture. During culture, no further hMSCs were introduced into the system.

2.13 RNA isolation and quantitative real time polymerase chain reaction (qRT-PCR)

Scaffolds were stored in RNAlater (Life Technologies). For analysis, homogenization of the cells was performed using lysis tubes with a Speed Mill P12 (both from Analytik Jena AG, Jena, Germany). Following centrifugation, RNA was isolated from supernatant using the innuSpeed RNA Mini Isolation kit (Analytik Jena AG). Transcription was done employing the Transcription First Strand cDNA Synthesis Kit (Roche Diagnostics). Only RNA-samples with a RIN-number of 9.0–10 were used. Quantitative real-time PCR (qRT-PCR) was performed with the QuantiFast SYBR Green qRT-PCR Kit (Qiagen, Hilden, Germany). Primers (Hs_ALPL_1_SG, Hs_BGLAP_1_SG, Hs_COL1A1_1_SG, Hs_GAPDH_2_SG, Hs_RUNX2_1_SG, Hs_SPP1_1_SG, Hs_SP7_1_SG, Hs_FAS1_SG, Hs_SERPINH1_1_SG, HS_SAFB_1_SG, Hs_GAPDH_2_SG and Hs_RPLP0_2_SG) were purchased from Qiagen. House-keeping genes *gapdh* and *rplp0* were used for normalization.

2.14 Data analysis

Statistical significant differences were assessed by the software OriginPro 8G, using the one factor analysis of variance (ANOVA) employing post hoc Fisher LSD test. Data were expressed as mean values ± standard deviation. *p*-values less than 0.05 were defined as statistically significant. *denotes a significant difference between two experimental groups (**p*<0.05; ***p*<0.01).

3 Results

3.1 Isolated human mesenchymal stem cells exhibit typical surface marker profile and multipotent differentiation capacity in two-dimensional culture

According to the International Society for Cell Therapy, different criteria should be applied for the characterization of stem cells. In addition to plastic adherence and expression of specific cell membrane proteins, the capacity to differentiate into adipocytes, osteoblasts and chondrocytes are required. hMSCs of four donors were analyzed by FACS to detect the antigen surface profile (Fig. 1A). CD73, CD90 and CD105 are known as positive marker proteins and were expressed in a consistency of >95%. The cell populations were negative for the surface antigens CD14, CD19, CD34 and CD45.

Differentiation of hMSCs was performed by medium supplementation revealing the capacity of osteogenic, adipogenic and chondrogenic lineage commitment. Results depicted in Fig. 1B–I are exemplarily shown for one donor (male, age 24). After 28 days of exposition to osteogenic medium, cells exhibited a strong calcium deposition, which was demonstrated by alizarin red staining (Fig. 1C). In contrast, no staining was observed in the negative control when cells were cultured in proliferation medium (Fig. 1B). Oilred O staining displayed a strong formation of cytoplasmic lipid droplets in hMSCs (Fig. 1E). No lipid droplets, and thus, no adipogenic differentiation were detected in the negative control, which was cultured in proliferation medium (Fig. 1D). The analysis of the chondrogenic differentiation in pellet cultures after 28 days was performed by collagen type II staining (Fig. 1F and 1G) and alcian blue (Fig. 1H and 1I). Alcian blue revealed prominent staining as well as collagen II and demonstrated chondrogenic lineage commitment, in contrast to pellets which were cultured in proliferation medium. Furthermore, osteogenic differentiation was analyzed by qRT-PCR measurement of *alpl*, *bglap*, *col1a1*, *runx2*, *spp1* after one and seven days of cell culture in proliferation medium and differentiation medium (Fig. 1J and 1K). Genes, known as early marker genes such as *alpl*, *col1a1* and *runx2* showed a higher gene expression after chemically induced osteogenesis compared to cells in proliferation medium. However, the statistical analysis revealed no significant induction of osteogenic related marker genes. Statistical significant decrease of gene level expression was detected for *bglap* (day one) and *spp1* (day seven).

3.2 Computational modeling predicts fluid mechanics

The perfusion bioreactor system was composed of the bioreactor cartridge confining the scaffold, a reservoir

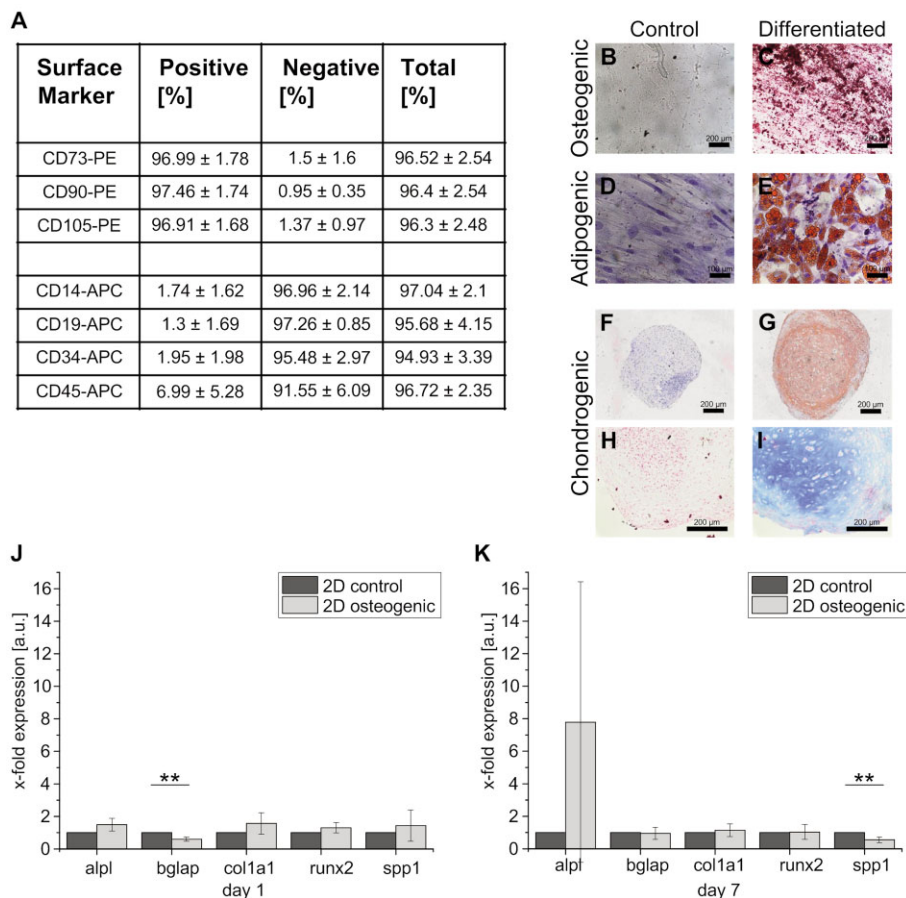


Figure 1. Characterization of human mesenchymal stem cells (hMSCs). (A) Fluorescence activated cell sorting (FACS) analysis depicts the average expression ± standard deviation of typical markers for human mesenchymal stem cells (hMSCs) of four different donors. (B, C) Osteogenic differentiation was demonstrated by alizarin red staining on day 28. (D, E) The formation of lipid droplets in adipogenic differentiated cells is shown by oil red O staining on day 14. The chondrogenic differentiation was performed by pellet cultures for 28 days and detected by histological staining of (F, G) col type II and (H, I) alcian blue to verify the expression of glycosaminoglycans. Cells cultured in proliferation medium were used as negative control. Exemplary images are shown from four independent experiments, including three replicates for each experiment. Expression of osteogenic related marker genes were analyzed by quantitative real time polymerase chain reaction (qRT-PCR) on (J) day one and (K) day seven. Gene levels of cells cultured in proliferation medium were used for normalization. Time-fold gene expression was normalized to the housekeeping gene *gapdh* and *rplp0* expression. *denotes a significant difference between culture conditions (* $p < 0.05$; ** $p < 0.01$). Error bars depict standard deviation. All results comprise the average data of four different donors, each donor includes three internal replicates.

flask, and an adapter for a pressure sensor (Fig. 2A). A peristaltic pump delivered cell culture medium from the reservoir flask to the bioreactor cartridge. The concept of the bioreactor cartridge (Fig. 2B) ensured homogeneous flow conditions inside the scaffold by pressing a silicone tube to the cylinder jacket surface of the porous polymer. Computational modeling of the bioreactor fluid dynamics allowed identifying the flow characteristics in the bioreactor and the resulting mechanical stimulation (Fig. 2C). The average mechanical shear stress at an inflow rate of 0.8 mL/min was calculated to 7.6×10^{-5} N/m². When not sealing the cylinder jacket surface of the scaffold, the average mechanical shear stress was reduced to 6.6×10^{-6} N/m² (Fig. 2D). The lower shear stress conditions resulted from a high volume flow in the gap between scaffold and housing. This also led to a heterogeneous perfu-

sion of the scaffold as depicted by the streamlines that are solely present inside the scaffold in the proximity of the in- and outlet.

3.3 Poly(L-lactide-co-caprolactone) scaffold material supports cell attachment

The P(LLA-co-CL) scaffold featured a cylindrical geometry with a diameter of 10.5 mm and 25 mm in height (Fig. 3A). μ CT analysis (Fig. 3B) and scanning electron microscopy (SEM; Fig. 3B) revealed a disordered and complex structure, exhibiting porous – porosity 90% –, highly interconnected material properties.

In order to show the capacity of the scaffolds to support attachment of hMSCs, cell material interaction was analyzed by immunofluorescence staining against actin

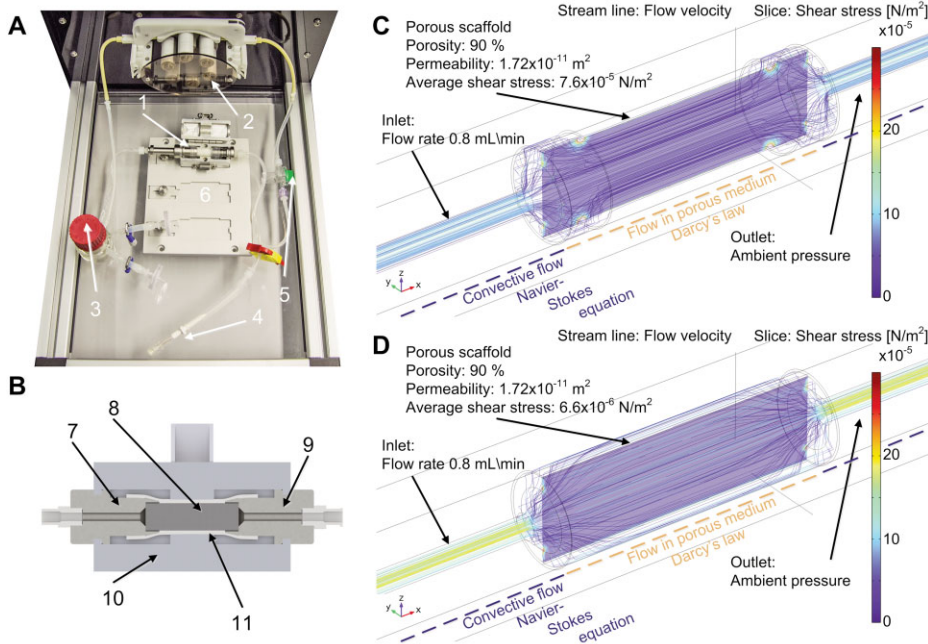


Figure 2. Bioreactor set up and computational modeling. **(A)** A bioreactor set up was composed of a bioreactor cartridge loaded with a poly(L-lactide-co-caprolactone) (P[LLA-co-CL]) scaffold (1), a computer-controlled pump (2), a reservoir flask including air filters (3), a septum for cell seeding (4), an adapter to attach a pressure sensor (5), and a rack system that allows easy handling (6). **(B)** A cross section shows the concept of the bioreactor cartridge. From an inlet (7), cell culture medium was guided through the cylindrical P[LLA-co-CL] scaffold (8) to an outlet (9). The bioreactor housing (10), pressed a silicone tube (11) to the cylinder jacket surface of the P[LLA-co-CL] scaffold to ensure homogeneous flow conditions in the scaffold. **(C)** Computational modeling depicts the fluid mechanical conditions in the bioreactor and scaffold. The average shear stress inside the scaffold was calculated to $7.6 \times 10^{-5} \text{ N/m}^2$. Due to the sealed cylinder jacket surface, all streamlines stayed within the scaffold. **(D)** In contrast, the open boundaries of the unsealed scaffold reduced the number of streamlines inside the scaffold to a minimum. Except from regions close to the in- and out-let, the scaffold was free of convective flow. This also resulted in low shear stress conditions of $6.6 \times 10^{-6} \text{ N/m}^2$, 10-fold lower compared to the radially sealed scaffold.

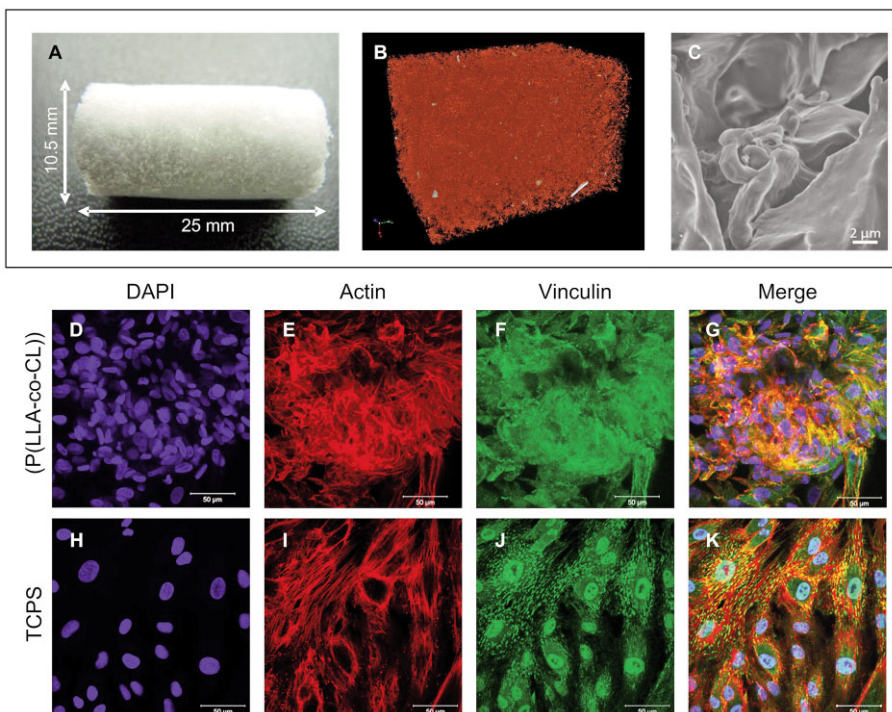


Figure 3. Characteristics of the applied material and evaluation of cell adhesion on the scaffold. **(A)** Macroscopic and **(B)** μ CT analysis, and **(C)** scanning electron microscopy (SEM) images of the poly(L-lactide-co-caprolactone) (P[LLA-co-CL]) scaffolds. From μ CT data, porosity was determined to 90%. Interconnectivity was characterized as 35 mm^2 in a total volume of 80 mm^3 . Approximately 99% of all pores were interconnected. To investigate cell material interaction, immunohistological stainings were performed and analyzed by laser scanning microscopy. **(D, H)** Cell nuclei were stained with DAPI (blue). To show cell adhesion and cell morphology of cells in the P[LLA-co-CL] scaffolds, fluorescence staining of **(E, I)** actin (red) and **(F, J)** vinculin (green), as a prominent component of focal adhesions, was performed ($n = 4$). Staining was conducted 48 h after seeding human mesenchymal stem cells (hMSCs) either into the cylindrical material or for comparison on standard tissue culture polystyrene (TCPS). **(G, K)** Merged images.

and vinculin. Focal adhesions were formed by cells adhered to the substrate. When comparing hMSCs attachment on P(LLA-co-CL) (Fig. 3 D–G) and standard cell culture flasks (Fig. 3 H–K), distribution of focal adhesion and actin filaments appeared more chaotic in the 3D culture due to the complex structure of the porous material, which also resulted in an apparently higher cell density.

3.4 Dynamic seeding and culture conditions result in homogenous cell distribution and induce mechanical stimulation

The closed bioreactor system, a peristaltic pump, and a pressure gauge were used to control seeding and culture

conditions. The reactor cartridge (Fig. 2A) sealed the scaffold and allowed perfusion through construct. 3-(4,5-dimethylthiazol-2-yl)-2,5-diphenyltetrazolium bromide (MTT) staining was performed on day one and seven to show cell viability and to analyze cell distribution within the material (Fig. 4A). Analysis of cross sectioned scaffolds at day seven revealed a homogenous cell distribution of viable cells throughout the scaffold for dynamic culture conditions, whereas cells in static conditions were restricted to the periphery of the scaffold. To analyze the influence of dynamic and static culture conditions on a molecular level, expression of stress-related genes was determined by qRT-PCR (Fig. 4B and 4C). Therefore, scaffolds were seeded with cells of each donor. The stress marker genes *fas* and *safb* in dynamic culture conditions

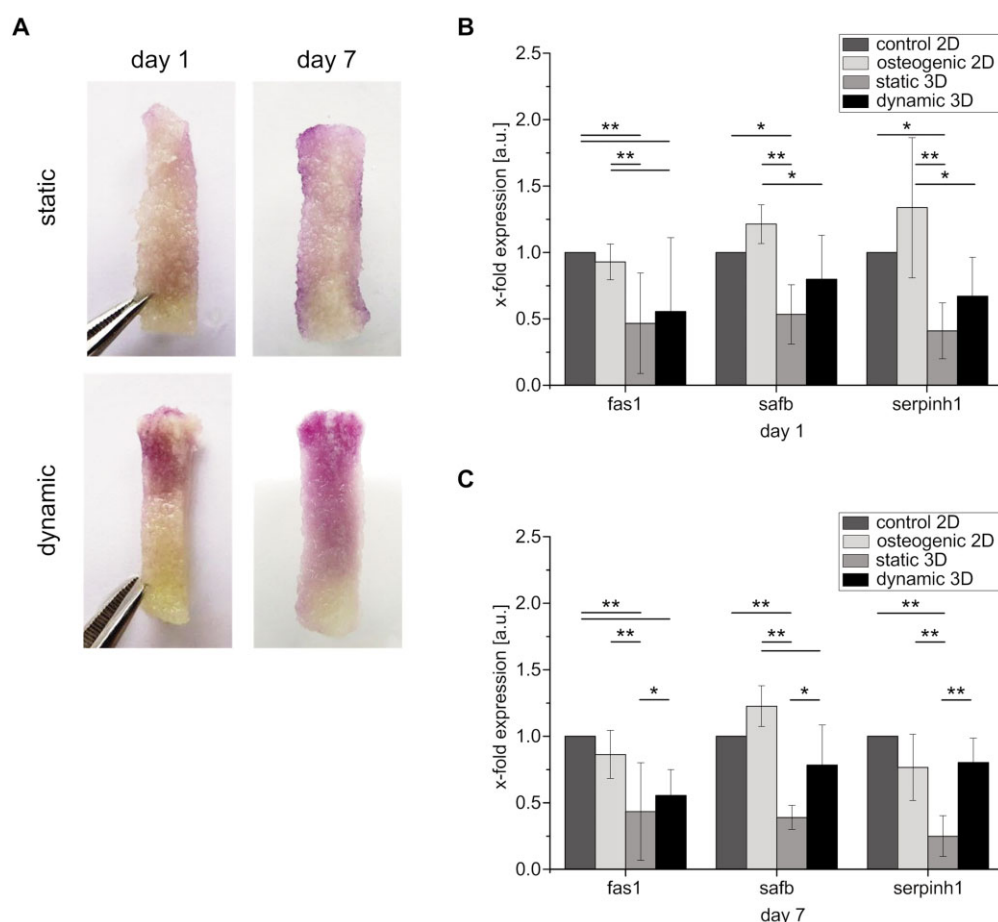


Figure 4. Evaluation of seeding efficacy and regulation of stress related genes within the scaffolds. (A) 3-(4,5-dimethylthiazol-2-yl)-2,5-diphenyltetrazolium (MTT) staining revealed the distribution of viable cells within the polymer scaffold after one and seven days. Cylinders were seeded employing an oscillating flow of 1.6 mL/min for 1 h. Following, statically cultured controls were placed in a glass bottle occupied with cell culture medium without flow conditions, whereas dynamically cultured samples were perfused applying a constant flow of 0.8 mL/min for 7 days. (B, C) Samples were analyzed by quantitative real time polymerase chain reaction (qRT-PCR) for detection of genes related to stress markers (*fas1*, *safb*, *serpinh1*). Housekeeping genes *gapdh* and *rplp0* were used for normalization. Furthermore, time-fold gene expressions were normalized to control cells in standard two-dimensional (2D) culture conditions. Legend: Control 2D: human mesenchymal stem cells (hMSCs) on standard tissue culture polystyrene using proliferative medium; Osteogenic 2D: hMSCs on standard tissue culture polystyrene using osteogenic differentiation medium; Static 3D: hMSCs in the 3D polymer scaffold using proliferative medium; Dynamic 3D: hMSCs in the 3D polymer scaffold exposed to shear stress employing the bioreactor system (n = 4). *denotes a significant difference in gene level expression between culture conditions (* $p < 0.05$; ** $p < 0.01$), error bars represent standard deviation.

were up-regulated compared to static culture conditions on day one. The expression rate of *saib* and *fas* turned out to be significantly up-regulated after seven days of dynamic culture in comparison to static culture conditions. On day seven, also *serpinh1* exposed a significantly higher up-regulation in dynamic conditions compared to static culture. For comparison, neither *saib*, *fas*, nor *serpin* showed significant differences between proliferation and osteogenic medium on day one and day seven. Interestingly, in the 3D culture system, except from *serpinh1* on day seven, all measured stress markers were lower compared to the standard two-dimensional (2D) culture conditions for all experimental settings.

3.5 Dynamic culture conditions induce calcification and up-regulation of osteogenic gene expression

To investigate the influence of dynamic culture conditions on osteogenic lineage commitment, alizarin red staining was performed for static and dynamic culture

conditions and both time points (Fig. 5A). Cell-loaded scaffolds cultured for seven days, exhibited stronger calcification than constructs that were cultured for one day. For quantification, a calcification assay was conducted (Fig. 5B). The quantification verified an increase of calcification from day one to day seven. Additionally, a significant difference was detected between static and dynamic culture conditions for day seven. For comparison, cell-free scaffolds control exhibited a readout of 0.23 ± 0.008 [a. u.].

To confirm these findings, qRT-PCR was performed. In dynamic culture conditions, except from *bglap*, osteogenic-related genes that are known to be up-regulated in early stages of the osteogenic differentiation process, were higher expressed at day one (Fig. 5C). On day seven, *bglap* was still decreased for the dynamically cultured cells compared to the static control and *alpl* was down-regulated in comparison to day one (Fig. 5D). On day one, *alpl* showed significantly higher values compared to the static cultured cells. This was also seen for *col1a1*, *runx2*, and *spp1*. Two times higher expression at day one and

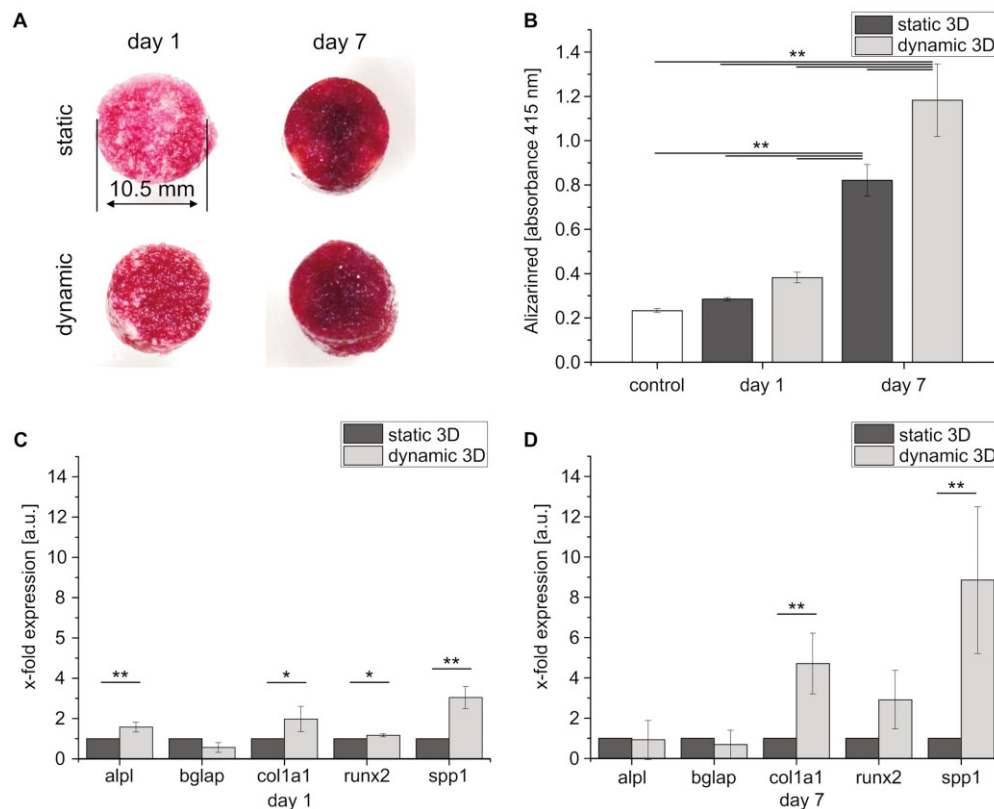


Figure 5. Osteogenic differentiation in a three-dimensional (3D) construct. Human mesenchymal stem cells (hMSCs) were cultured for one or seven days in proliferation medium under static or dynamic culture conditions. (A) Alizarin red staining was used to analyze mineralization. (n = 4) (B) Calcium concentration was measured quantitatively by dissolving alizarin red. Furthermore, times-fold gene expression was measured by quantitative real time polymerase chain reaction (qRT-PCR). Osteogenesis related genes were analyzed at (C) day one and at (D) day seven. *denotes a significant difference between culture conditions (* $p < 0.05$; ** $p < 0.01$). Error bars depict standard deviation. Data are shown as average from four different donors, each donor comprises three internal replicates.

five times higher expression at day seven was observed for *col1a1*. *runx2* turned out to be three times higher in the dynamic culture in comparison to the static control on day seven. The three-fold higher expression of *spp1* on day one increased to a nine-fold higher value on day seven, when comparing static and dynamic culture.

4 Discussion

Tissue-engineered bone grafts are considered as an alternative treatment for critical size bone defects [3, 4]. The minimal dimension of a critical size bone defect depends on the organism. For mice, 4 mm defect size was identified as critical [21], rabbit defect critical sizes should exhibit a length of 6 mm, and larger animal models more than 12 mm [22]. In our study, P(LLA-co-CL) cylinders with a diameter of 10.5 mm and a length of 25 mm were used as scaffolds to meet the requirements for critical size defects in large animals and humans [23].

Several studies indicated improved bone formation of synthetic bone substitutes when the material is seeded with cells before implantation [3, 24]. For cell seeding, different strategies such as incubation in cell suspension [16, 25] or centrifugation [26] were described. Furthermore, shaking was claimed to allow high seeding efficiency with uniformly distributed cells within a scaffold [27]. We establish a seeding protocol employing bioreactor technology allowing homogeneous distribution of hMSCs in cylindrical scaffolds.

In previous studies, oscillating flow for seeding has already been described as beneficial regarding cell viability [28, 29]. However, for the P(LLA-co-CL) scaffolds, optimal parameters had to be identified. In contrast to previously published protocols, scaffold seeding was already accomplished after 1 h in comparison to 2 h. Further, the seeding parameters exhibited a higher dynamic in terms of flow velocity (0.15 or 1.0 mL/min vs. 1.6 mL/min) and oscillating frequency (5 min vs. cycles for 10 s forward and 3 s backward). From a technological point of view, our seeding process was performed fully automatically without manual intervention. Furthermore, pressure was controlled during seeding. Efficient seeding could be demonstrated on day one. After seven days of dynamic culture, an almost homogenous cell distribution, even in the core region of the cylinder was found. MTT staining of the cross-sectioned scaffolds showed viable cells after seven days of exposure to perfusion. We concluded that the identified flow rate of 0.8 mL/min during culture results in a sufficient nutrients supply and waste product removal. At higher flow rates, we observed decreased cell densities, probably due to cell death. This correlates to previously published data by Cartmell et al. [25]. Furthermore, we analyzed the apoptosis marker *fas* and detected an increased gene level expression on day one, compared to statically cultured scaffolds. After seven days of flow

exposure, the gene level expression remained on similar levels and did not increase further. In contrast to static culture conditions, the expression profile of *serpinh1*, which is correlated to general stress (Heat shock protein 47) [30], is highly up-regulated on day one and seven, and displays the effect of shear stress to the cells. Up-regulation was also detected for the stress marker *saib*, the scaffold attachment factor B, which contributes in stress regulation and in differentiation processes. We decided to monitor this marker, which is described as intermediary in shear-induced signals and is up-regulated in response to fluid shear stress in endothelial cells [31]. We observed a significant up-regulation of gene expression at day seven in fluid-stress-exposed cells. Interestingly, when comparing stress marker levels of cells in the 2D and 3D culture, gene level expression was lower in 3D for all experimental conditions, except *serpinh1* at day seven. The 3D culture environment and the material parameters seem to provide more physiological conditions in terms of i.e. mechanical properties [10], cell orientation (Fig. 3) or cell communication via soluble factors compared to the 2D culture [32]. Nevertheless, introduction of flow into the 3D construct increases stress marker expression levels.

Although high cell densities are achievable and low stress marker levels are observed in the bioreactor system, the construct nutrient supply will be impaired after implantation in absence of convection due to size of the construct. In native bone, the periosteum, which is highly vascularized, provides nutrients to the bone tissue. Thus, for future work, strategies for introducing artificial periosteum tissue are required. Nevertheless, direct perfusion in the bioreactor can be employed further to trigger specific lineage commitment.

In the bioreactor system, perfusion leads to shear stress that triggers cell differentiation [33]. Osteogenic lineage commitment was demonstrated qualitatively by alizarin red staining. Previous studies have already shown an increased expression of bone markers in osteoblast-like cells that were cultured statically in P(LLA-co-CL) scaffolds [10, 34]. The significantly higher calcification in dynamic culture conditions in comparison to static culture conditions shows that the developed bioreactor system allows to further strengthen osteogenic lineage commitment. To support these findings, gene level expression was investigated. Induction of osteogenic differentiation results in up-regulation of osteogenic marker genes including collagen 1A1 (*col1a1*), alkaline phosphatase (*alpl*), *runx* related factor 2 (*runx2*), osteonectin (*sparc*), and osteocalcin (*bglap*) [35]. Our data evince that shear stress, evoked by perfusion, increases the expression of these osteogenesis related genes. On day one, the expression of quiet early regulated genes as *alpl*, *runx2*, *col1a1*, and *spp1* was higher in dynamically cultured compared to statically cultured cells. Strongest up-regulation was detected for *spp1* on day one and day seven. Osteopontin was described to have a crucial role in bone remodeling

processes in response to mechanical stress, the high up-regulation of *spp1* can be attributed to shear stress in dynamical culture [36]. In previous studies which employed shear stress in addition to supplementation of dexamethasone and ascorbic phosphate into the cell culture medium, increased osteogenic expression patterns were detected [18, 25]. Interestingly, mechanical induction of osteogenic lineage commitment exhibits higher cell compatibility, when comparing expression of stress markers of cells that were differentiated with soluble factors and cells that were cultured in the bioreactor.

The developed bioreactor technology allows the generation of cell-loaded bone substitutes for treatment of critical size bone defects by overcoming limitations of nutrients supply in a complex 3D scaffold. The dynamic culture conditions enhance calcification and expression of osteogenic related genes after one week of culture. Without adding growth factors, solely by mechanical stimulation, early osteogenic lineage commitment was achieved. The omission of soluble factors supports the development of processes compliant to GMP guidelines, and may accelerate technology translation in clinical applications.

Our work was funded by the European Union's Seventh Framework Program, grant agreement number 242175-VascuBone and by the BMBF Förderaktivität, "New Methods in Systems Biology – SysTec", grant agreement number 0315506D.

The authors declare no financial or commercial conflict of interest.

5 References

- [1] Bohner, M., Design of ceramic-based cements and putties for bone graft substitution. *Eur. Cell Mater.* 2010, 20, 1–12.
- [2] Holzapfel, B. M., Chhaya, M. P., Melchels, F. P., Holzapfel, N. P. et al., Can bone tissue engineering contribute to therapy concepts after resection of musculoskeletal sarcoma? *Sarcoma* 2013, 2013, 153640.
- [3] Viateau, V., Guillemin, G., Bousson, V., Oudina, K. et al., Long-bone critical-size defects treated with tissue-engineered grafts: A study on sheep. *J. Orthop. Res.* 2007, 25, 741–749.
- [4] Kon, E., Muraglia, A., Corsi, A., Bianco, P. et al., Autologous bone marrow stromal cells loaded onto porous hydroxyapatite ceramic accelerate bone repair in critical-size defects of sheep long bones. *J. Biomed. Mater. Res.* 2000, 49, 328–337.
- [5] Mistry, A. S., Mikos, A. G., Tissue engineering strategies for bone regeneration. *Adv. Biochem. Eng. Biotechnol.* 2005, 94, 1–22.
- [6] Bose, S., Roy, M., Bandyopadhyay, A., Recent advances in bone tissue engineering scaffolds. *Trends Biotechnol.* 2012, 30, 546–554.
- [7] Khan, W. S., Rayan, F., Dhinsa, B. S., Marsh, D., An osteoconductive, osteoinductive, and osteogenic tissue-engineered product for trauma and orthopaedic surgery: How far are we? *Stem Cells Int.* 2012, 2012, 236231.
- [8] Krudwig, W. K., Anterior cruciate ligament reconstruction using an alloplastic ligament of polyethylene terephthalate (PET – Trevira – hochfest). Follow-up study. *Biomed. Mater. Eng.* 2002, 12, 59–67.
- [9] Hutmacher, D. W., Scaffolds in tissue engineering bone and cartilage. *Biomaterials* 2000, 21, 2529–2543.
- [10] Idris, S. B., Arvidson, K., Plikk, P., Ibrahim, L. et al., Polyester copolymer scaffolds enhance expression of bone markers in osteoblast-like cells. *J. Biomed. Mater. Res.* 2010, 94A, 631–639.
- [11] Danmark, S., Finne-Wistrand, A., Wendel, M., Arvidson, K. et al., Osteogenic Differentiation by Rat Bone Marrow Stromal Cells on Customized Biodegradable Polymer Scaffolds. *J. Bioact. Compat. Polym.* 2010, 25, 207–223.
- [12] Novosel, E. C., Kleinhans, C., Kluger, P. J., Vascularization is the key challenge in tissue engineering. *Adv. Drug Deliv. Rev.* 2011, 63, 300–311.
- [13] Liu, L., Zong, C., Li, B., Shen, D. et al., The interaction between beta1 integrins and ERK1/2 in osteogenic differentiation of human mesenchymal stem cells under fluid shear stress modelled by a perfusion system. *J. Tissue Eng. Regen. Med.* 2012, 8, 85–168.
- [14] Lim, K. T., Kim, J., Seonwoo, H., Chang, J. U. et al., Enhanced osteogenesis of human alveolar bone-derived mesenchymal stem cells for tooth tissue engineering using fluid shear stress in a rocking culture method. *Tissue Eng. Part C Methods* 2013, 19, 128–145.
- [15] Sikavitsas, V. I., Bancroft, G. N., Mikos, A. G., Formation of three-dimensional cell/polymer constructs for bone tissue engineering in a spinner flask and a rotating wall vessel bioreactor. *J. Biomed. Mater. Res.* 2002, 62, 136–148.
- [16] Stiehler, M., Bunger, C., Baatrup, A., Lind, M. et al., Effect of dynamic 3-D culture on proliferation, distribution, and osteogenic differentiation of human mesenchymal stem cells. *J. Biomed. Mater. Res.* 2009, 89, 96–107.
- [17] Wang, T. W., Wu, H. C., Wang, H. Y., Lin, F. H., Sun, J. S., Regulation of adult human mesenchymal stem cells into osteogenic and chondrogenic lineages by different bioreactor systems. *J. Biomed. Mater. Res.* 2009, 88A, 935–946.
- [18] Barron, M. J., Goldman, J., Tsai, C. J., Donahue, S. W., Perfusion flow enhances osteogenic gene expression and the infiltration of osteoblasts and endothelial cells into three-dimensional calcium phosphate scaffolds. *Int. J. Biomater.* 2012, 2012, 915620.
- [19] Hansmann, J., Groeber, F., Kahlig, A., Kleinhans, C., Walles, H., Bioreactors in tissue engineering – principles, applications and commercial constraints. *Biotechnol. J.* 2013, 8, 298–307.
- [20] Raeth, S., Sacchetti, B., Siegel, G., Mau-Holzmann, U. A. et al., A mouse bone marrow stromal cell line with skeletal stem cell characteristics to study osteogenesis in vitro and in vivo. *Stem cells Dev.* 2014, 23, 1097–1108.
- [21] Harris, J. S., Bemenderfer, T. B., Wessel, A. R., Kacena, M. A., A review of mouse critical size defect models in weight bearing bones. *Bone* 2013, 55, 241–247.
- [22] Pearce, A. I., Richards, R. G., Milz, S., Schneider, E., Pearce, S. G., Animal models for implant biomaterial research in bone: A review. *Eur. Cells Mater.* 2007, 13, 1–10.
- [23] Szpalski, C., Barr, J., Wetterau, M., Saadeh, P. B., Warren, S. M., Cranial bone defects: Current and future strategies. *Neurosurg. Focus* 2010, 29, E8.
- [24] Hesse, E., Kluge, G., Atfi, A., Correa, D. et al., Repair of a segmental long bone defect in human by implantation of a novel multiple disc graft. *Bone* 2010, 46, 1457–1463.
- [25] Cartmell, S. H., Porter, B. D., Garcia, A. J., Guldberg, R. E., Effects of medium perfusion rate on cell-seeded three-dimensional bone constructs in vitro. *Tissue Eng.* 2003, 9, 1197–1203.
- [26] Ng, R., Gurm, J. S., Yang, S. T., Centrifugal seeding of mammalian cells in nonwoven fibrous matrices. *Biotechnol. Prog.* 2010, 26, 239–245.
- [27] Jones, G., Cartmell, S. H., Optimization of cell seeding efficiencies on a three-dimensional gelatin scaffold for bone tissue engineering. *J. Appl. Biomater. Biomech.* 2006, 4, 172–180.

- [28] Alvarez-Barreto, J. F., Sikavitsas, V. I., Improved mesenchymal stem cell seeding on RGD-modified poly(L-lactic acid) scaffolds using flow perfusion. *Macromol. Biosci.* 2007, 7, 579–588.
- [29] Du, D., Furukawa, K. S., Ushida, T., 3D culture of osteoblast-like cells by unidirectional or oscillatory flow for bone tissue engineering. *Biotechnol. Bioeng.* 2009, 102, 1670–1678.
- [30] Mala, J. G., Rose, C., Interactions of heat shock protein 47 with collagen and the stress response: An unconventional chaperone model? *Life Sci.* 2010, 87, 579–586.
- [31] Li, S., Piotrowicz, R. S., Levin, E. G., Shyy, Y. J., Chien, S., Fluid shear stress induces the phosphorylation of small heat shock proteins in vascular endothelial cells. *Am. J. Physiol.* 1996, 271, C994–1000.
- [32] Alepee, N., Bahinski, A., Daneshian, M., De Weyer, B. et al., State-of-the-art of 3D cultures (organs-on-a-chip) in safety testing and pathophysiology. *ALTEX*- 2014, 31, 441–477.
- [33] Rodrigues, C. A., Fernandes, T. G., Diogo, M. M., da Silva, C. L., Cabral, J. M., Stem cell cultivation in bioreactors. *Biotechnol. Adv.* 2011, 29, 815–829.
- [34] Sun, Y., Xing, Z., Xue, Y., Mustafa, K. et al., Surfactant as a critical factor when tuning the hydrophilicity in three-dimensional polyester-based scaffolds: Impact of hydrophilicity on their mechanical properties and the cellular response of human osteoblast-like cells. *Biomacromolecules* 2014, 15, 1259–1268.
- [35] Doi, M., Nagano, A., Nakamura, Y., Genome-wide screening by cDNA microarray of genes associated with matrix mineralization by human mesenchymal stem cells in vitro. *Biochem. Biophys. Res. Commun.* 2002, 290, 381–390.
- [36] Ishijima, M., Tsuji, K., Rittling, S. R., Yamashita, T. et al., Osteopontin is required for mechanical stress-dependent signals to bone marrow cells. *J. Endocrinol.* 2007, 193, 235–243.



Cover illustration

This regular issue of BTJ features articles on the production of biofuels, small molecules and recombinant proteins. The cover is inspired by an article describing increased expression levels of recombinant proteins in potato tubers upon post-harvest light treatment. © Lenslife – Fotolia.com

Biotechnology Journal – list of articles published in the November 2015 issue.

Editorial

Biotechnology Journal brings more than biotechnology

Alois Jungbauer and Sang Yup Lee

<http://dx.doi.org/10.1002/biot.201500581>

Meeting Report

Plant Science Student Conference (PSSC) 2015 –

Young researchers in green biotechnology

Susann Mönchgesang, Christoph Ruttkies, Hendrik Treutler and Marcus Heisters

<http://dx.doi.org/10.1002/biot.201500393>

Commentary

Development of a high affinity Affibody-derived protein against amyloid β -peptide for future Alzheimer's disease therapy

Erwin De Genst and Serge Muyldermans

<http://dx.doi.org/10.1002/biot.201500405>

Review

The long-lasting love affair between the budding yeast *Saccharomyces cerevisiae* and the Epstein-Barr virus

María José Lista, Cécile Voisset, Marie-Astrid Contesse, Gaëlle Friocourt, Chrysoula Daskalogianni, Frédéric Bihel, Robin Fåhræus and Marc Blondel

<http://dx.doi.org/10.1002/biot.201500161>

Mini-Review

Micro 3D cell culture systems for cellular behavior studies: Culture matrices, devices, substrates, and in-situ sensing methods

Jonghoon Choi, Eun Kyu Lee, Jaebum Choo, Junhan Yuh and Jong Wook Hong

<http://dx.doi.org/10.1002/biot.201500092>

Review

Outer membrane vesicles as platform vaccine technology

Leo van der Pol, Michiel Stork and Peter van der Ley

<http://dx.doi.org/10.1002/biot.201400395>

Research Article

A truncated and dimeric format of an Affibody library on bacteria enables FACS-mediated isolation of amyloid-beta aggregation inhibitors with subnanomolar affinity

Hanna Lindberg, Torleif Hård, John Löfblom and Stefan Ståhl

<http://dx.doi.org/10.1002/biot.201500131>

Research Article

Enhanced glutathione production by evolutionary engineering of *Saccharomyces cerevisiae* strains

Anett Patzschke, Matthias G. Steiger, Caterina Holz, Christine Lang, Diethard Mattanovich and Michael Sauer

<http://dx.doi.org/10.1002/biot.201400809>

Research Article

A perfusion bioreactor system efficiently generates cell-loaded bone substitute materials for addressing critical size bone defects

Claudia Kleinhans, Ramkumar Ramani Mohan, Gabriele Vacun, Thomas Schwarz, Barbara Haller, Yang Sun, Alexander Kahlig, Petra Kluger, Anna Finne-Wistrand, Heike Walles and Jan Hansmann

<http://dx.doi.org/10.1002/biot.201400813>

Research Article

Biocatalyzed approach for the surface functionalization of poly(L-lactic acid) films using hydrolytic enzymes

Alessandro Pellis, Enrique Herrero Acero, Hansjoerg Weber, Michael Obersriebnig, Rolf Breinbauer, Ewald Srebotnik and Georg M. Guebitz

<http://dx.doi.org/10.1002/biot.201500074>

Research Article

A systematic analysis of TCA *Escherichia coli* mutants reveals suitable genetic backgrounds for enhanced hydrogen and ethanol production using glycerol as main carbon source

Antonio Valle, Gema Cabrera, Howbeer Muhamadali, Drupad K. Trivedi, Nicholas J. W. Ratray, Royston Goodacre, Domingo Cantero and Jorge Bolivar

<http://dx.doi.org/10.1002/biot.201500005>

Research Article

Engineering surface hydrophobicity improves activity of *Bacillus thermocatenuatus* lipase 2 enzyme

Ting Tang, Chongli Yuan, Hyun-Tae Hwang, Xuebing Zhao, Doraiswami Ramkrishna, Dehua Liu and Arvind Varma

<http://dx.doi.org/10.1002/biot.201500011>

Research Article

The potential of random forest and neural networks for biomass and recombinant protein modeling in *Escherichia coli* fed-batch fermentations

Michael Melcher, Theresa Scharl, Bernhard Spangl, Markus Luchner, Monika Cserjan, Karl Bayer, Friedrich Leisch and Gerald Striedner

<http://dx.doi.org/10.1002/biot.201400790>

Research Article

Determination of antibiotic EC₅₀ using a zero-flow microfluidic chip based growth phenotype assay

Jing Dai, Sang-Jin Suh, Morgan Hamon and Jong Wook Hong

<http://dx.doi.org/10.1002/biot.201500037>

Research Article

A potyvirus vector efficiently targets recombinant proteins to chloroplasts, mitochondria and nuclei in plant cells when expressed at the amino terminus of the polyprotein

Eszter Majer, José-Antonio Navarro and José-Antonio Daròs

<http://dx.doi.org/10.1002/biot.201500042>

Research Article

Post-harvest light treatment increases expression levels of recombinant proteins in transformed plastids of potato tubers

Luis M. Larraya, Alicia Fernández-San Millán, María Ancín, Inmaculada Farran and Jon Veramendi

<http://dx.doi.org/10.1002/biot.201500028>

Biotech Method

Prediction of reversible IgG1 aggregation occurring in a size exclusion chromatography column is enabled through a model based approach

Frida Ojala, Anton Sellberg, Thomas Budde Hansen, Ernst Broberg Hansen and Bernt Nilsson

<http://dx.doi.org/10.1002/biot.201500160>

Biotech Method

Dual lifetime referencing enables pH-control for oxidoreductions in hydrogel-stabilized biphasic reaction systems

Jens Begemann and Antje C. Spiess

<http://dx.doi.org/10.1002/biot.201500198>